Low energy electron beam top surface image processing using chemically amplified AXT resist

C. S. Whelan and D. M. Tanenbaum[a)]
School of Applied and Engineering Physics, Cornell University, Ithaca, New York 14853

D. C. La Tulipe
SRDC, IBM Thomas J. Watson Research Center, Yorktown Heights, New York 10598

M. Isaacson and H. G. Craighead
School of Applied and Engineering Physics, Cornell University, Ithaca, New York 14853

(Received 28 May 1997; accepted 26 August 1997)

High resolution processes are demonstrated with a positive-mode chemically amplified AXT top surface imaging resist system exposed with a low energy electron beam. Top surface imaging is an ideal match to low energy electron beam lithography because it allows thick resist layers to be patterned despite the limited penetration depth of the electron beam. The three key steps of the process are exposure, silylation, and etch development. All three steps influence the final process sensitivity, contrast, and resolution. The AXT has a poly(hydroxy styrene) base resin, and has been formulated both with and without a dye used to enhance optical absorption. We have achieved sub 100 nm resolution both with and without a postexposure bake. Critical area doses below 1 μC/m^2 are demonstrated. The edge roughness and density of etch residue from silylation defects have been compared for a variety of oxygen plasma etch systems. © *1997 American Vacuum Society.*
[S0734-211X(97)16406-X]

I. INTRODUCTION

As optical lithography moves towards deep-ultraviolet (DUV), wavelengths, top surface imaging (TSI) has been promoted as a method to achieve high resolution processing of thick planarizing resist layers with limited optical penetration. In pursuing viable processes for massively parallel low energy electron beam microcolumn lithography, we have previously examined a variety of multilayer and ultrathin single layer resist processes.[1–3] These processes are necessary because of the limited penetration depth of low energy electrons. The benefit of the limited penetration is the elimination of proximity effects associated with backscattering of electrons from the substrate. The first negative-tone TSI process for low energy electron beam lithography was demonstrated by MacDonald *et al.*[4] Böttcher *et al.* have demonstrated that positive-tone TSI can be effective for low energy electron beam lithography with a novolac based resist.[5] Our work expands on positive-tone low energy electron beam lithography with AXT, a poly(hydroxy styrene) (PHOST) resin based chemically amplified resist, coupled with extremely high aspect ratio etch processing.[6] The chemical amplification allows the sensitivity of the resist to be raised orders of magnitude higher than the base resin. Pure PHOST resin has been studied extensively as a model TSI resist system for use with 193 nm optical projection lithography.[7] High sensitivity is needed to achieve high throughput in any direct write electron beam lithography scheme, such as arrays of low energy microcolumns.[8] Similar to multilayer processes, top surface imaging combined with selective silylation and all dry plasma development processes allows for high resolution patterning of thick resist layers independent of underlying topography.

Positive- and negative-tone TSI processes have been extensively studied, particularly using novolac based resists, for high resolution optical lithography.[9,10] Chemically amplified, novolac based SAL-601 has been exposed with high energy electron beam lithography[11,12] and focused ion beam lithography[13] for TSI. In TSI, silicon is selectively incorporated from vapor[14] or liquid[15,16] sources into the exposed or unexposed regions of a single layer resist for negative or positive processes, respectively. The silicon incorporation occurs via diffusion and chemical reaction between the silylating agent and resist, from the top surface downward. Temperature, concentration, and time for silylation can be controlled to limit the depth of the silicon incorporation. The thin patterned silicon containing layer is then ''developed'' in an all dry oxygen plasma etch. An etch resistant SiO_x layer is formed in silylated regions, while unsilylated regions etch quickly in the O_2 plasma regardless of cross linking.

TSI processes are similar to bilayer and multilayer processes which also incorporate thin imaging layers over a bulk resist. One advantage over such processes is that the resist is still a single layer prior to the silylation step, and can be spin coated in a single step. A second advantage is that because the etch resistant silicon is added after the exposure, it does not have any effect on the penetration depth or scattering of incident low energy electrons. This is a significant advantage as electron energies are reduced below 1 keV and penetration depths are $\sim$50 nm.[2] It also appears that thin silylated resist layers suffer fewer pinhole-type defects than comparable spin coated polymer films. Typically TSI processes have problems with unwanted silylation in open regions that result

[a)]Present address: Physics Department, Pomona College, 610 N. College Ave., Clarement, CA 91711-6359; Electronic mail: dtanenbaum@POMONA.edu

in etch ''grass'' residues from the highly selective oxygen plasma development.[17]

AXT resist consists of a PHOST base resin with a photoacid generator and a cross linker. It was prepared in two forms; one with a highly absorbing anthracene dye, one without the dye. The resist solvent was propylene glycol methyl ether acetate (PGMEA). The cross linker is known to catalyze some reactions even at room temperature in the presence of the photoacid. AXT has been demonstrated as a cost effective system for DUV lithography, and is compatible with a mix and match processing of DUV and electron beam exposures.

II. EXPERIMENT

Wafers were spin coated with AXT at 5000 rpm for 60 s and pre-baked for 60 s at 128 °C on a vacuum hot plate. The resulting resist thickness was 1.2 μm. The coated sample was then exposed at 2 keV (except where noted) using a modified Leo/Zeiss 982 DSM field emission microscope. The scanning of the beam was remotely controlled by a home built pattern generator. Immediately following exposure the patterned sample was postexposure baked (PEB) at 125 °C for 120 s. No postexposure bake was also investigated. The sample was then silylated in either a Genesis 200 system or a custom built silylating chamber at 115 °C and 30 Torr for roughly 40 s using dimethylsilyldiethylamine (DMSDEA). These silylation parameters resulted in a resist swell of 80–100 nm as measured by a profilometer, or an interferometer with a fixed index of refraction, $n = 1.59$. To transfer the latent silylated image into the bulk of the resist three types of oxygen reactive ion etchers (RIE) were characterized; PlasmaTherm SSL-720 conventional RIE, LAM transformer coupled plasma (TCP), and a PlasmaQuest electron cyclotron resonance (ECR). The resist was characterized at different processing steps using the low voltage scanning electron microscope (SEM), Rutherford backscattering (RBS), and Fourier transform infrared spectroscopy (FTIR).

III. SILYLATION PROCESS

Vapor pressure and silylation time were used as control parameters to determine the degree of silylation in open (unexposed) regions. In these regions the $SiH(CH_3)_2$ from the DMSDEA replaces the proton in the hydroxyl group on the PHOST causing a swell of the resist, in addition to incorporating the silicon. The increase in thickness (swell) was recorded and used to characterize the silylation process for AXT as a function of pressure, time, and postexposure treatment. In the exposed regions the PHOST is cross linked restricting the polymer relaxation necessary to allow DMSDEA diffusion. The chemical contrast of the process as a function of dose is shown in Fig. 1. Novolac based resists such as SAL-601 are often treated with a pre-silylation development step to reduce the flow of low T_g silylated material over the cross linked (exposed) regions.[9,11,18] With PHOST based AXT, the flow of the silylated material appears to be less of a problem, although some silylation does occur in the exposed regions.

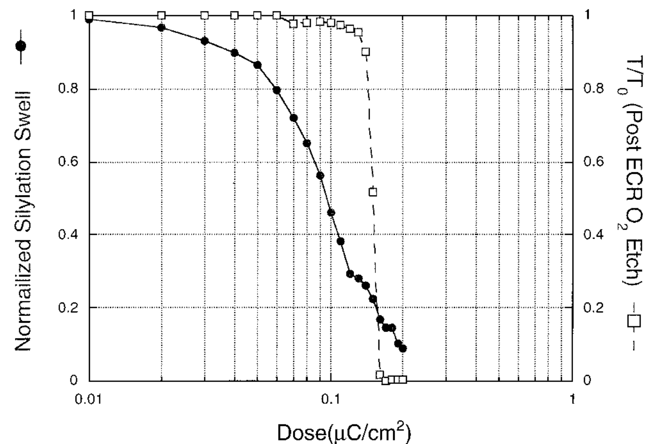

FIG. 1. Normalized silylation swell (before final etch) and resist thickness (after final etch) vs dose for 2 keV exposure of AXT resist (no dye) using a 125 °C PEB. The full silylation swell is 65 nm, and the total resist thickness is 1.19 μm.

The silylation has been characterized by cross sectional imaging with a low voltage SEM which reveals the relationship between the swell and the depth of the silylation. The images are taken after cleaving through silylated patterns. The silylation profile can be enhanced by a brief O_2 RIE normal to the cleaved surface. No conductive coating is introduced. Cross sections of a deeply silylated sample are shown in Fig. 2. The swell in large unexposed regions is

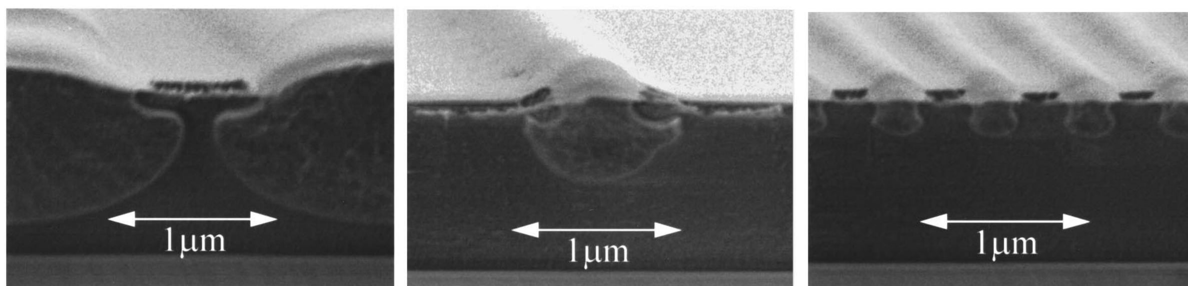

FIG. 2. Cross sectional SEM images of the silylation profiles of an isolated line, an isolated space, and higher resolution features written at 2 keV. All images are from the same silylation run, showing the undercutting of the cross linked region and feature size dependent silylation depth.

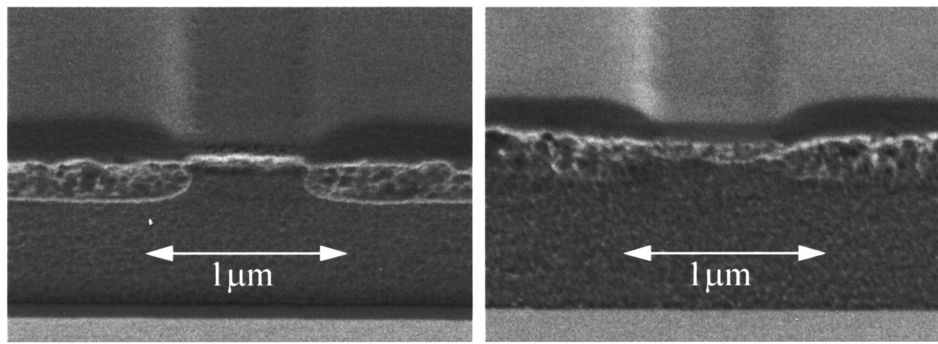

FIG. 3. Two cleaved cross sectional SEM images of the same isolated line exposure. The left one has been enhanced by an edge on O_2 RIE. There is significant roughness present independent of the RIE enhancement. No conductive coating was applied, and the samples are tilted 45° and 51°, respectively.

~30% of the silylated layer thickness. The silylation is typically modeled as a non-Fickian, case II diffusion.[14] The cross sections show the silylation depth is dependent upon feature size, as has been seen in optical exposures of the resist.[6] In contrast to optical exposures, the shallow penetration depth of low energy electrons allows deep silylations to undercut exposed isolated lines.

The SEM images show a highly nonuniform texture in the silylated regions. Nonuniformity in the silylated areas has been proposed as one source of the edge roughness of the dry developed resist profile, a result of the high selectivity of the RIE as the silylation mask erodes at the edge.[19] To ensure that this apparent nonuniformity was not due to the edge on O_2 RIE, we examined samples directly after the cleave of the silylated layer. As seen in Fig. 3, there is substantial roughness both in the silylated and unsilylated regions of the resist, with dimensions of ~100 and ~50 nm, respectively.

FTIR and RBS have been used to examine a series of samples ranging from no silylation to near complete silylation. The FTIR absorption data show a steady decrease of the hydroxyl peak (~3390 cm^{-1}), a small rise in the Si–H peak (~2135 cm^{-1}), and a large increase at the ph–O–Si peak (~920 cm^{-1}) as a function of increasing silylation time. Figure 4 shows FTIR and RBS data for a typical silylation run. RBS shows the silicon incorporation is fairly uniform in the silylated layer, converting ~70% of the hydroxyl sites. From the RBS the silylated layer is ~12% Si by weight (~3% atomic conc.)

IV. ETCHING

A conventional oxygen RIE was initially used to transfer the silylated latent image into the full thickness of resist. When bombarded with oxygen ions the silylated resist forms SiO_x and becomes resilient to further erosion. Conversely the e-beam exposed area of the resist, which contains no silicon, is vertically etched to the substrate below. Typical parameters for the RIE etch were 40 sccm of O_2, 10 mTorr, 30 °C, and −400 V dc bias. The results of this etch are shown in Fig. 5. The sidewalls appear near vertical due to the anisotropy of the etch, but are very rough. Large amounts of uniformly distributed ''grass'' are also evident in the open regions. This grass comes from multiple sources; defects due to sputtering of the SiO_x mask, acid neutralization at the surface of the exposed areas from airborne amines result in insufficient cross linking and therefore silylation, and partial silylation in cross linked regions despite inhibited diffusion. The RIE cannot remove the defects from the acid neutralization nor from the partial silylation because of the low ion density in the plasma. The large dc bias typical of RIE leads to sputtering of the SiO_x into the open regions.

For these reasons a high density, low bias LAM TCP was investigated. A nonselective ''pre-burn'' etch consisting of 40 sccm oxygen, 2 mTorr, 350 W source power, 350 W chuck power, and 0 °C was used to remove the top 10–15 nm of the entire film. This aides in removing the unwanted

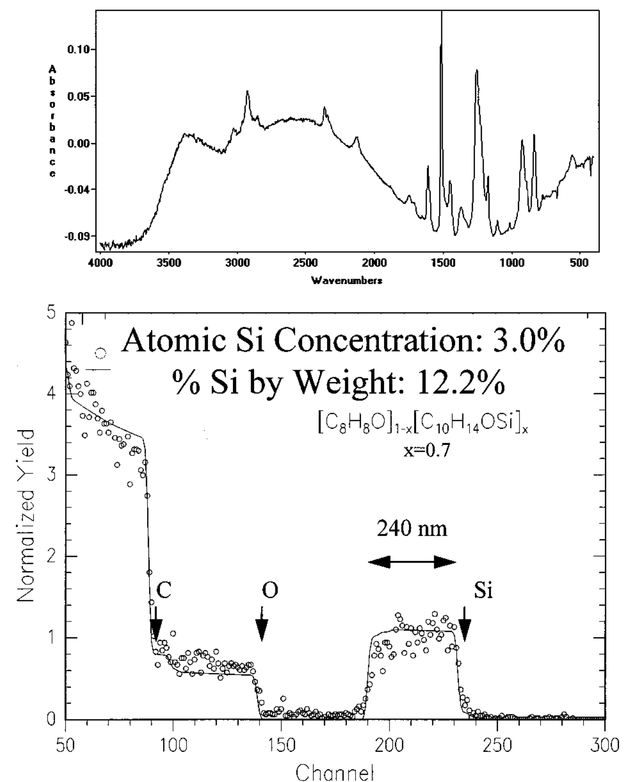

FIG. 4. FTIR absorbance spectra and RBS data for the same silylated (unexposed) sample of AXT resist (no dye.) The silylation swell (depth) is 65 nm (240 nm).

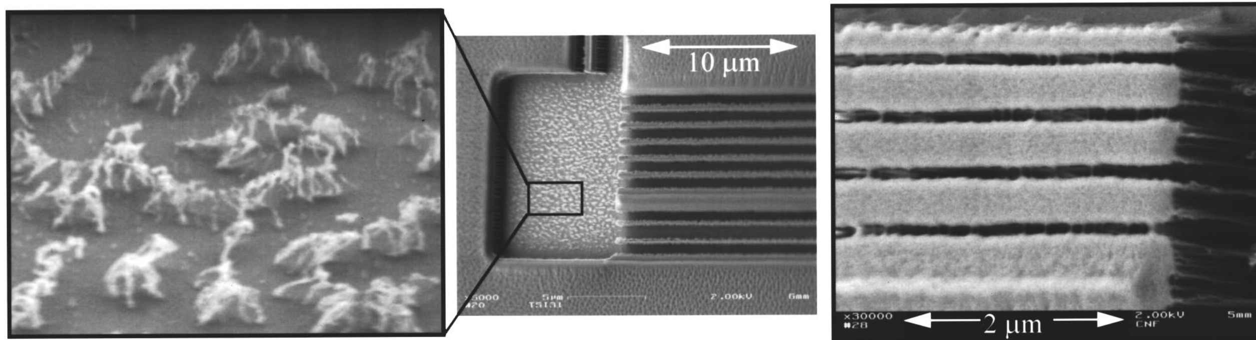

FIG. 5. Results of conventional RIE etch development following silylation of patterns written in AXT at 2 keV.

silylation in exposed areas. Following this short etch, the chuck power and the source power were reduced to 150 and 220 W, respectively, and the sample was etched to completion using CO end point detection.[6] Typical results from this etch are shown near the critical dose in Fig. 6. The high ion density plasma and the pre-burn step were effective in removing most of the defects, but some remain near the edges of the open region. Because of the proximity to the edges of the open region we can hypothesize that this is a result of the still high dc bias. Although not directly measurable, the dc bias resulting from 150 W of chuck power remains approximately comparable to the RIE. The sidewalls appear smoother than the RIE, but are slightly bowed near the critical dose. At higher doses the sharply defined cross linking/silylation boundary results in perfectly vertical sidewalls since the low temperature virtually eliminates the horizontal etch component.[20]

In an attempt to reduce sputtering further, an ECR etch was developed. Chamber pressure, oxygen flow, upper magnet power, lower magnet power, and chuck temperature were set fixed from screening experiments at 5 mTorr, 40 sccm, 16.4 A, 100 A, and 20 °C, respectively. Source and chuck power were varied over a large range. Optimum selectivity of 40:1 is obtained with 700 W microwave power and 50 W source power. This rf source power combination results in a relatively low bias of ~ -100 V which reduces sputtering of

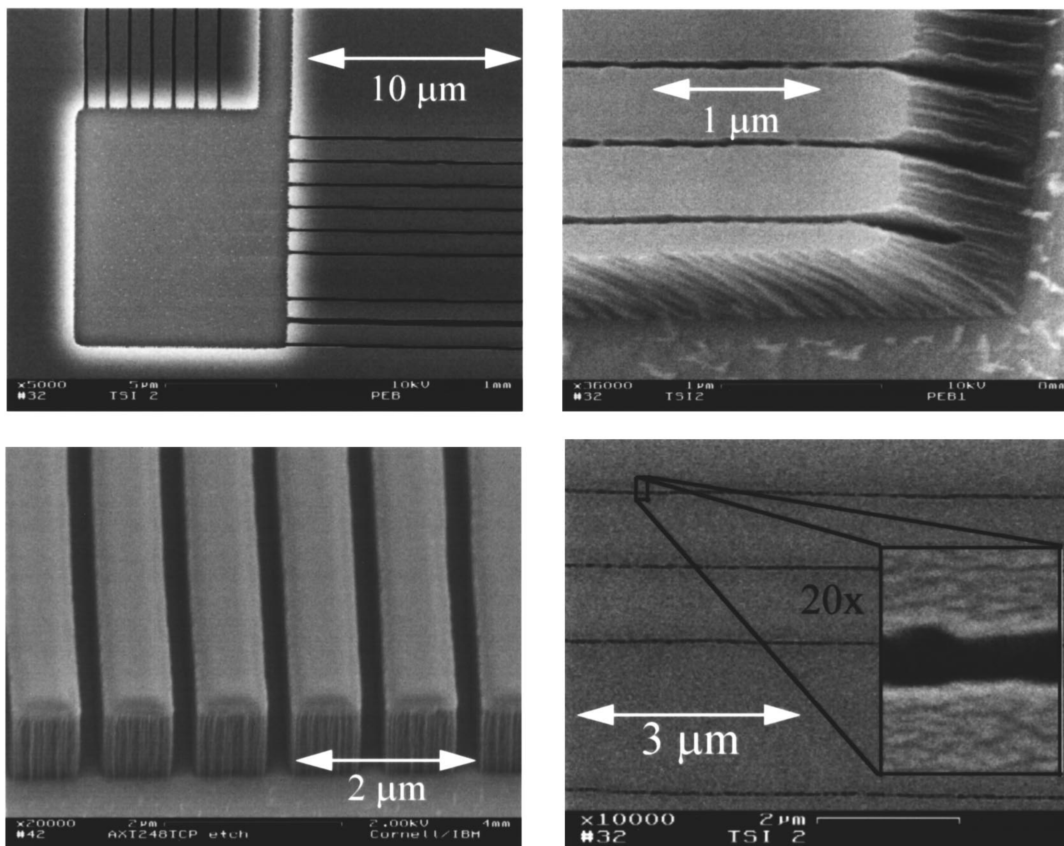

FIG. 6. Results of TCP RIE etch development following silylation of patterns written in AXT at 2 keV.

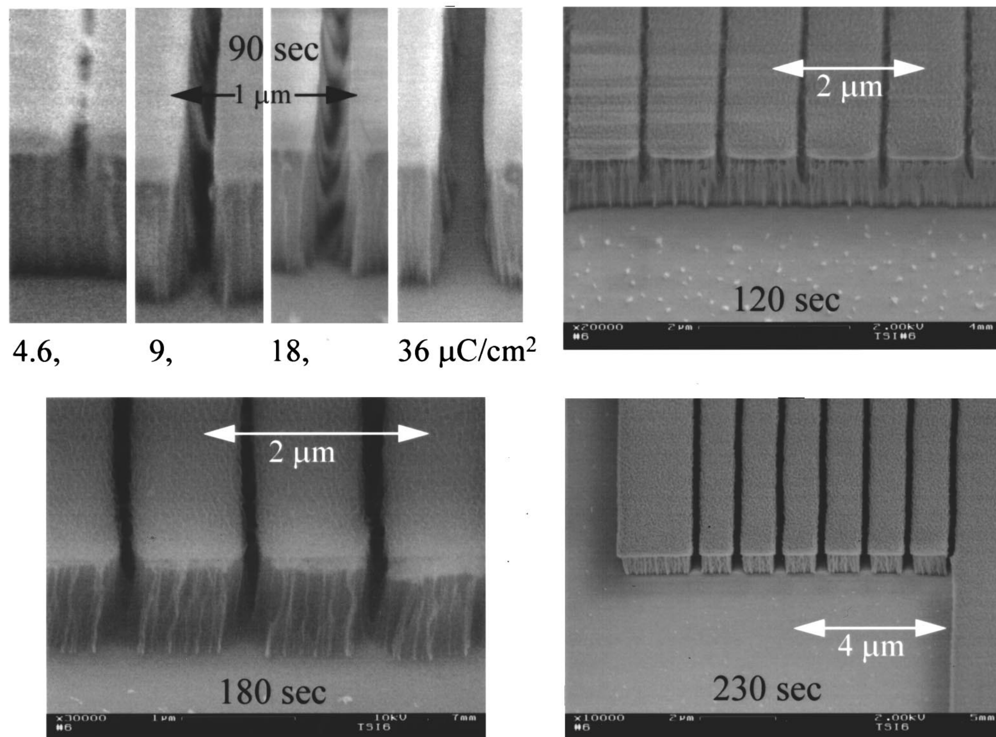

FIG. 7. Results of ECR RIE etch development following silylation of patterns written in AXT at 2 keV. Image (a) shows a range of doses for a 90 s etch, images (b–d) show etch times of 120, 180, and 230 s, respectively.

the mask into the open regions, and the high ion density plasma is effective in removing most of the silylation defects in exposed regions. The remaining grass is quite small. Typical results near the critical dose are shown in Fig. 7. Edge roughness is comparable to the TCP etch but takes on a different appearance. Profiles are also near vertical when etched to completion, but overetching results in *T* topping. In contrast the features over etched in the TCP (particularly during the pre-burn) get wider due to mask erosion, but remain vertical due to the low temperature. When silylation mask cross sections are compared with ECR plasma developed patterns we find close correlation, as seen in Fig. 8. This is a result of the high etch selectivity and rounded silylation profile which provides etch process latitude.

V. EXPOSURE

As seen in Fig. 1, the critical dose with PEB, a silylation swell of 65 nm, and 120 s ECR etch development is $\sim 0.2\ \mu C/cm^2$. In contrast, the critical dose of AXT under similar conditions but without PEB is $\sim 30\ \mu C/cm^2$. Even without the 125 °C PEB, the samples are subjected to a 115 °C hot plate during silylation. The 10 °C shift is responsible for the increased sensitivity showing the chemical amplification process is very sensitive to temperature. We do not find a significant difference in sensitivity when comparing AXT with and without the dye. The efficiency of the chemical amplification can be seen by comparing it with the critical dose of pure PHOST resin, $\sim 600\ \mu C/cm^2$, under similar conditions.[21] There is a substantial interplay between exposure energy, dose, silylation depth, and etch time which determine the critical dose. The critical doses reported are representative of a reliable portion of parameter space.

For all electron beam exposures, the minimum feature size increases with dose partially due to the Gaussian beam profile. In addition we expect broadening of features due to acid diffusion in chemically amplified resist systems. Preliminary measurements of single pass linewidth as a function of dose show substantial broadening of features processed with the PEB. Single pass lines (5 keV) processed without a PEB show a reduced widening which appears to plateau at ~ 100 nm.

VI. RESULTS

In comparison with the optical exposures of AXT, we find several distinctive characteristics of electron beam exposures. The silylating agent can undercut the cross linked resist, reducing the positive tone feature size below the dimensions of the cross linked regions. This has not been observed in exposures of AXT by either 248 or 193 nm light. In analyzing the edge roughness of maskless exposures, we find no significant improvement over the edge roughness observed in optical mask based lithography.[6] Thus the roughness is inherent to either the silylation or etch conditions, but not the mask edge roughness. The acid diffusion present in the chemically amplified resist, which should smooth the interface between the cross linked and unexposed regions, does not smooth the developed edge roughness. Attempts to re-

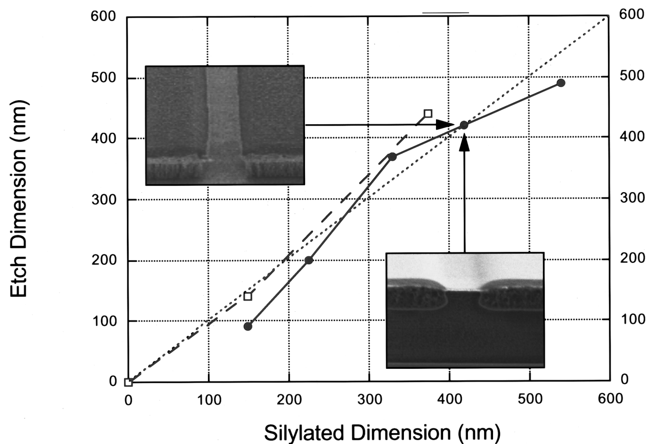

FIG. 8. Patterned etch dimension vs silylated dimension cross sections for a series of isolated lines and isolated spaces.

duce the edge roughness by over etching or variation in silylation depth do not improve upon the observed edge roughness.

The observed resolution of the AXT TSI system for 2 keV electron beam exposures is ~50 nm as can be seen in Fig. 6. This is comparable to the resolution of our 2 keV exposures of poly(methylmethacrylate) (PMMA). This resolution was achieved with a PEB which includes acid diffusion broadening and a single pass linear exposure dose of 13 pC/cm. The silylation profile did not undercut the cross linked resist. If sensitivity is not an issue, the PEB temperature can be reduced in exchange for high resolution process stability.

To demonstrate the utility of AXT we used a SF_6/Cl_2 ECR plasma etch to transfer the resist pattern into bulk silicon. The selectivity of Si:AXT was 1.5:1. An aspect ratio of 12:1 was achieved with nearly vertical sidewalls and linewidths of 150 nm.

VII. SUMMARY

The AXT chemically amplified, TSI positive-tone PHOST based resist system can be effectively patterned with 2 keV electrons with sub 100 nm resolution and a sensitivity below 1 $\mu C/cm^2$. Silylation with DMSDEA shows rounded silicon mask edge, with ~3% atomic [Si] in the mask. A high density ECR oxygen plasma development can be effectively utilized with no pre-burn or fluorine based chemistry, resulting in vertical resist sidewalls and minimal etch residue.

AXT has already demonstrated 193 nm optical TSI lithography resolution of 150 nm, making it a viable candidate for the next generation of semiconductor fabrication. We have now demonstrated that this same resist system can also be patterned with low energy electron beam lithography with a minimum feature size (line or space) ~50 nm. A future generation of fabrication could use mixed and matched optical and low energy electron beam lithography using the single AXT TSI resist system.

ACKNOWLEDGMENTS

The authors wish to recognize several researchers who helped in this effort. Discussions with A. Gabor stimulated the research program. D. Seeger made the collaboration between IBM and Cornell possible. P. Revesz performed the RBS measurements. D. Carr, M. Hupcey, R. Davis, G. Feit, M. Horn, C. Nelson, and R. Kunz all supported our research efforts by openly sharing their expert advice. This work was supported by DARPA. Portions of the work were performed at the Cornell Nanofabrication Facility and the Cornell Materials Science Center that are supported in part by the National Science Foundation.

[1] C. W. Lo, M. J. Rooks, W. K. Lo, M. Isaacson, and H. G. Craighead, J. Vac. Sci. Technol. B **13**, 812 (1995).
[2] C. W. Lo, W. K. Lo, M. J. Rooks, M. Isaacson, H. G. Craighead, and A. E. Novembre, J. Vac. Sci. Technol. B **13**, 2980 (1995).
[3] D. M. Tanenbaum, C. W. Lo, M. Isaacson, H. G. Craighead, M. J. Rooks, K. Y. Lee, W. S. Huang, and T. H. P. Chang, J. Vac. Sci. Technol. B **14**, 3829 (1996).
[4] S. A. MacDonald, L. A. Pederson, A. M. Patlach, and C. G. Wilson, Proc. ACS Symp. **346**, 350 (1987).
[5] M. Böttcher, L. Bauch, and I. Stolberg, J. Vac. Sci. Technol. B **12**, 3473 (1994).
[6] D. C. La Tulipe, J. P. Simons, and D. E. Seeger, Proc. SPIE **2195**, 372 (1994). See also US Patent No. 5,322,765 (21 June 1994).
[7] R. R. Kunz, S. C. Palmateer, M. W. Horn, A. R. Forte, and M. Rothschild, Proc. ACS Symp. **614**, 271 (1995).
[8] T. H. P. Chang, M. G. R. Thompson, E. Kratschmer, H. S. Kim, M. L. Yu, K. Y. Lee, S. A. Rishton, B. W. Hussey, and S. Zolgharnain, J. Vac. Sci. Technol. B **14**, 3774 (1996).
[9] E. Pavelchek, G. Calabrese, B. Dudley, S. Jones, P. Freeman, J. Bohland, and R. Sinta, Proc. SPIE **1925**, 264 (1993).
[10] A. M. Goethals, K. H. Baik, K. Ronse, J. Vertommen, and L. V. d. hove, Proc. SPIE **2195**, 394 (1994).
[11] M. Irmscher, B. Höflinger, and R. Springer, Proc. SPIE **2724**, 564 (1996).
[12] M. Irmscher, B. Höflinger, and R. Springer, J. Vac. Sci. Technol. B **12**, 3925 (1994).
[13] M. A. Hartney, D. C. Shaver, M. I. Shepard, J. Melngailis, V. Medvedev, and W. P. Robinson, J. Vac. Sci. Technol. B **9**, 3432 (1991).
[14] M. A. Hartney, J. Vac. Sci. Technol. B **11**, 681 (1993).
[15] K. H. Baik, K. Ronse, L. V. d. hove, and B. Roland, Proc. SPIE **1925**, 302 (1993).
[16] K. Maeda, T. Ohfuji, N. Aizaki, and E. Hasegawa, Proc. SPIE **2438**, 465 (1995).
[17] J. Hutchinson, Y. Meaku, W. Nguyen, and S. Das, Proc. SPIE **2724**, 399 (1996).
[18] W. S. Han, J. H. Lee, J. C. Park, C. G. Park, H. Y. Kang, Y. B. Koh, and M. Y. Lee, Proc. SPIE **1925**, 291 (1993).
[19] C. Nelson (personal communication).
[20] S. C. Palmateer, R. R. Kunz, M. W. Horn, A. R. Forte, and M. Rothschild, Proc. SPIE **2438**, 455 (1995).
[21] D. M. Tanenbaum and A. H. Gabor (unpublished).